

Investigations of the Antibacterial Properties of Ciprofloxacin@SiO₂

M. J. Rosemary,[†] Ian MacLaren,^{‡,§} and T. Pradeep^{*,†}

DST Unit on Nanoscience, Department of Chemistry and Sophisticated Analytical Instrument Facility, Indian Institute of Technology, Madras, Chennai 600 036, India, and Department of Physics and Astronomy, University of Glasgow, Glasgow G12 8QQ, United Kingdom

Received May 19, 2006. In Final Form: August 10, 2006

The antibacterial activity of ciprofloxacin-encapsulated silica nanoshells synthesized from gold@silica core–shell nanoparticles has been investigated. The minimum inhibitory concentration of the material was found using the agar dilution method, and it showed better antibacterial activity compared to free ciprofloxacin in the case of *Escherichia coli* DH5 α , whereas the same activity was found for *Lactococcus lactis* MG 1363. Hydrophobicity measurements carried out in an octanol–water mixture suggested that ciprofloxacin@SiO₂ is distributed almost equally in the aqueous and nonaqueous phases. The kinetics of the uptake of ciprofloxacin@SiO₂ was compared with that of free ciprofloxacin. Fluorescence imaging studies carried out using fluorescein isothiocyanate@SiO₂ showed that the nanoshells enter the bacterial cell. The uptake of silica shells has been probed by transmission electron microscopy also.

Introduction

Core–shell particles are very important because of their applications in areas such as catalysis, cancer diagnosis, and sensors.^{1–4} When the core of these particles is removed or when a thin shell is made over an inert core, the material obtained is called a nanoshell.^{5–9} Recently, the focus of attention has been on gold and silver metal nanoshells principally due to their use in the fields of cancer diagnosis and therapy.¹⁰ Nanoshells made of oxides such as silica and titania find application in the field of drug delivery. The outer surface of these shells can be used for attaching antibodies so that the silica shell–antibody complex can be used for targeted drug delivery in biological systems.¹¹ The existing drug delivery systems can be categorized into two groups, namely, the polymer- and lipid-based systems, in which the drugs are incorporated into or attached to the polymer or lipid.^{12–14} An important difference between the two groups is that the lipid-based systems often suffer from the problem of instability while the polymer-based systems are normally more

stable. The lipid-based systems are normally more biocompatible than the polymer-based systems as lipids belong in the human body.

In the recent past there has been considerable interest in nanosystems such as gold nanoparticles, carbon nanotubes, etc. for drug delivery applications. There have been numerous reports in this area, and it may not be necessary to list them all here. However, it may be noted that vancomycin-protected gold nanoparticles showed an increased microbial activity as compared to the free drug.¹⁵ Increased antibacterial activity of drugs incorporated inside liposomes compared to the free drug was reported previously by Desiderio and Campbell.¹⁶ It was reported that the uptake of single-walled carbon nanotube–streptavidin conjugates into human promyelocytic leukemia cells (HL60) and human T cells (Jurkat) is possible through endocytosis.¹⁷ It was in this context that we thought of investigating the antibacterial properties of ciprofloxacin@SiO₂; the synthesis and characterization of this material were reported by our group previously.^{18,19}

Ciprofloxacin is a fluoroquinolone synthetic antimicrobial agent whose primary mechanism of action against microorganisms involves inhibition of topoisomerase IV and DNA gyrase.²⁰ It has been widely used against urinary tract infections,²¹ bacterial prostatitis,²² sexually transmitted diseases,^{12,23} and joint,²⁴ skin and soft tissue,²⁵ respiratory tract,²⁶ and gastrointestinal²⁷ infections. It has been found that ciprofloxacin is active against

* To whom correspondence should be addressed. E-mail: pradeep@iitm.ac.in. Fax: 00-91-44-2257-0509 or 0545.

[†] Indian Institute of Technology.

[‡] University of Glasgow.

[§] At the Institute for Materials Science, Darmstadt University of Technology, Petersenstrasse 23, 64287 Darmstadt, Germany, while this work was initiated.

(1) Kakuta, N.; Park, K. H.; Finlayson, M. F.; Veno, A.; Bard, A. J.; Campion, A.; Fox, M. A.; Webber, S. E.; White, J. M. *J. Phys. Chem.* **1985**, *89*, 3828–3833.

(2) Nasr, C.; Chandini, H. S.; Kim, W. Y.; Schmehl, R. H.; Kamat, P. V. *J. Phys. Chem. B* **1997**, *101*, 7480–7487.

(3) Yuping, B.; Krishnan, K. M. *J. Magn. Mater.* **2005**, *293*, 15–19.

(4) Ren, X.; Meng, X.; Fangjiong, T. *Sens. Actuators, B* **2005**, *110*, 358–363.

(5) Makarova, O. V.; Ostafin, A. E.; Miyoshi, H.; Norris, J. R. Jr.; Meisel, D. *J. Phys. Chem. B* **1999**, *103*, 9080–9084.

(6) Ostafin, A. E.; Siegel, M.; Wang, Q.; Mizukami, H. *Microporous Mesoporous Mater.* **2003**, *57*, 47–55.

(7) Hirsch, L. R.; Jackson, J. B.; Lee, A.; Halas, N. J.; West, J. L. *Anal. Chem.* **2003**, *75*, 2377–2381.

(8) Jackson, J. B.; Westcott, S. L.; Hirsch, L. R.; West, J. L.; Halas, N. J. *Appl. Phys. Lett.* **2003**, *82*, 257–259.

(9) Loo, C.; Hirsch, L. R.; Lee, M.; Chang, E.; West, J. L.; Halas, N. J.; Drezek, R. *Opt. Lett.* **2005**, *30*, 1012–1014.

(10) Loo, C.; Lowery, A.; Halas, N. J.; West, J.; Drezek, R. *Nano Lett.* **2005**, *5*, 709–711.

(11) Wong, C.; Burgess, J. P.; Ostafin, A. E. *J. Young Investigators* **2002**, *6*, 3–4.

(12) Guo, X.; Szoka, F. C., Jr. *Acc. Chem. Res.* **2003**, *36*, 335–341.

(13) Furneri, P. M.; Fresta, M.; Puglisi, G.; Tempera, G. *J. Antimicrob. Chemother.* **2000**, *44*, 2458–2464.

(14) Ha, C. S.; Gardella, J. A., Jr. *J. Chem. Rev.* **2005**, *105*, 4205–4232.

(15) Gu, H.; Ho, P. L.; Tong, E.; Wang, L.; Xu, B. *Nano. Lett.* **2003**, *3*, 1261–1263.

(16) Desiderio, J. V.; Campbell, S. G. *J. Infect. Dis.* **1983**, *148*, 563–570.

(17) Kam, N. W. S.; Jessop, T. C.; Wender, P. A.; Dai, H. *J. Am. Chem. Soc.* **2004**, *126*, 6850–6851.

(18) Rosemary, M. J.; Suryanarayanan, V.; Reddy, P. G.; MacLaren, I.; Baskaran, S.; Pradeep, T. *Proc.—Indian Acad. Sci., Chem. Sci.* **2003**, *115*, 703–709 (Prof. C. N. R. Rao Special Issue).

(19) Tom, R. T.; Suryanarayanan, V.; Reddy, P. G.; Baskaran, S.; Pradeep, T. *Langmuir* **2004**, *20*, 1909–1914.

(20) Wolfson, J. S.; Hooper, D. C. *Clin. Microbiol. Rev.* **1989**, *2*, 378–424.

(21) Sanders, W. E., Jr. *Rev. Infect. Dis.* **1988**, *10*, 528–543.

(22) Guibert, J.; Destree, D.; Konopka, C.; Acar, J. *Eur. J. Clin. Microbiol.* **1986**, *5*, 247–248.

(23) Roddy, R. E.; Handsfield, H. H.; Hook, E. W., III. *Antimicrob. Agents Chemother.* **1986**, *30*, 267–269.

(24) Scott, G. R.; McMillan, A.; Young, H. *J. Antimicrob. Chemother.* **1987**, *20*, 117–121.

(25) Eron, L. J.; Harvey, L.; Hixon, D. L.; Poretz, D. M. *Antimicrob. Agents Chemother.* **1985**, *27*, 308–310.

both Gram-positive and Gram-negative bacteria. A broad-spectrum antibiotic is so-called due to its activity against a wide range of infectious agents.

Ciprofloxacin@SiO₂ (cip@SiO₂) has been synthesized as described in our previous paper.¹⁸ The starting point of the synthesis is Au@ciprofloxacin.¹⁹ The synthesized nanoshell has been characterized using UV-vis spectroscopy, fluorescence spectroscopy, and electron microscopy. The interaction of the material with both Gram-positive and Gram-negative bacteria was looked at. To make a comparison of the antimicrobial activity of the material with that of the free drug, the minimum inhibition concentrations (MICs) were found and showed almost the same value for the free drug and the drug incorporated inside the silica shell. The accumulation studies were conducted using a modified method described by Mortimer and Piddock.²⁸ We have also looked at the hydrophobicity of this newly made material to find possible ways it interacts with the bacterial cell. A fluorescence imaging experiment was carried out using fluorescein isothiocyanate (FITC) incorporated inside a silica nanoshell, FITC@SiO₂, as FITC has fluorescence in the visible region and is used widely in biology for imaging.^{29,30} Our investigations show that nanoshells are incorporated inside the bacterial cell. Ultrathin sections of *Escherichia coli* treated with cip@SiO₂ were analyzed using transmission electron microscopy (TEM).

Experimental Section

Bacteria and Growth Conditions. The bacterial strains used were *E. coli* DH5 α (Gram-negative bacteria) and *Lactococcus lactis* MG 1363 (Gram-positive bacteria). *E. coli* was cultured in LB (Luria-Bertani) medium at 37 °C, while *L. lactis* was cultured in M 17 broth at 30 °C. *E. coli* DH5 α and *L. lactis* MG 1363 were purchased from Life Technologies and Bioneer, Denmark, respectively.

Media and Materials. Ciprofloxacin was purchased from Fluka. Chloroauric acid, trisodium citrate, and octanol were purchased from CDH Fine Chemicals, India. (3-Aminopropyl)methyldiethoxysilane (APS), fluorescein isothiocyanate, and tetramethoxysilane (TMS) were purchased from Aldrich and were used without additional purification. Ethanol and 2-propanol were purchased from E. Merck. Carbon tetrachloride and glutaraldehyde were purchased from Ranbaxy Chemicals, India. Tryptone, yeast extract, sodium chloride, peptic digestase of animal tissue, peptic digestase of soy bean meat, yeast extract, beef extract, ascorbic acid, magnesium sulfate, lactose, disodium β -glycerophosphate, glucose, and agar were purchased from Hi-Media Chemicals, India. OsO₄, uranyl acetate, and lead citrate were purchased from Electron Microscopy Sciences.

The synthesis of cip@SiO₂ has been reported previously.¹⁸ A brief synthetic protocol is given in the Supporting Information, p 1. Various experimental tools were used to characterize it. The presence of ciprofloxacin inside the shells was confirmed by leaching experiments.

Determination of the MIC. The MIC was determined using the agar dilution method, which is a common method used for this purpose.³¹ Cultures grown to the mid-log phase were taken and diluted to get around 1000 organisms/mL approximately. They were mixed with different concentrations (μ g/mL) of cip@SiO₂/free

ciprofloxacin solutions and were incubated for 3 h at 37 °C for *E. coli* and at 30 °C for *L. lactis*. After 3 h, 1 mL of each culture was spread onto an agar plate and was incubated for 48 h. The MIC was determined by the observation of growth on the plate.

Measurement of the Rate of Accumulation of Quinolones by *E. coli* DH5 α and *L. lactis* MG 1363. The modified fluorescence method, as described by Mortimer and Piddock,²⁸ was used for measuring the concentration of cip@SiO₂/free ciprofloxacin accumulated for *E. coli* and *L. lactis*. A starter culture was added to 50 mL of the LB medium/M17 broth and grown to the mid-log phase of both the strains at 37 °C/30 °C. The OD was checked by keeping the wavelength at 600 nm. After centrifugation at 10000 rpm for 10 min, the pellet obtained was washed with 0.1 M sodium phosphate at pH 7.0 and was concentrated to make a suspension with an A₆₀₀ equivalent to 5 U. Ciprofloxacin/cip@SiO₂ was added to get a final concentration of 5 μ g/mL and was incubated at 37 °C/30 °C with *E. coli*/*L. lactis*, respectively, for 3 h. A 0.1 mL portion of the sample was withdrawn at definite time intervals starting from $t = 0$ and was washed with the phosphate buffer. Cell lysis was done by boiling the solution for 10 min. The solutions were centrifuged, and the supernatant was made up to 3 mL for the fluorescence measurements. The fluorescence intensity was monitored at 458 nm (for an excitation of 323 nm).

Instrumentation. Cip@SiO₂ was characterized using UV-vis spectroscopy, fluorescence spectroscopy, and transmission electron microscopy. UV-vis absorption spectra were recorded using a Perkin-Elmer Lambda 25 spectrometer. Emission spectra were measured using an F-4500 Hitachi spectrofluorimeter and Jobin-Vyon fluorolog instrument. The band-pass for excitation and emission was set as 5 nm. The fluorescence image was taken using a confocal Raman microscope of WiTec, Germany. The 514.5 nm line of an Ar ion laser was used for excitation, the spectrum was measured using a Peltier-cooled CCD detector, and the spectrometer was operated in the backscattering geometry. A 100 \times objective was used for selecting the area of interest. Transmission electron microscopy specimens of the nanoshell solutions were made by dropping the solution onto a holey carbon grid and allowing them to dry. These grids were imaged using a JEOL 3010 UHR transmission electron microscope equipped with a Gatan imaging filter. For imaging biological samples, ultrathin sections were made using a Leica EM UC 6 and were analyzed using a JEOL 3010 transmission electron microscope with 100 kV electrons.

Ultramicrotomy. Samples for ultramicrotomy were made by fixing *E. coli* treated with cip@SiO₂ in 1% glutaraldehyde for 1 $\frac{1}{2}$ h followed by washing the samples four times using Sorenson's phosphate buffer in a cold bucket^{32,33} followed by postfixation using 1% OsO₄ for 1 $\frac{1}{2}$ h.³⁴ Washing was done again four times using Sorenson's phosphate buffer in a cold bucket. This was followed by dehydration with 50%, 70%, and 100% acetone solutions. Infiltration was done by using Araldite and toluene in different ratios, followed by embedding. The embedded samples were cut using a diamond knife to a thickness of 80 nm and were collected on copper grids. The sections taken on the grid were stained first by 1% uranyl acetate for 3 h. The grids were washed using 100%, 70%, 50%, and 30% methanol followed by 100% water in succession. Lead citrate was used for further staining for 10 min, and washings were done first in 1 N sodium hydroxide followed by triply distilled water. The grids were then dried by keeping them on filter paper.

Results and Discussion

Silica nanoshells were synthesized as described in ref 18 from core-shell gold silica particles using sodium cyanide as well as CCl₄ as leaching agents.³⁵ As characterization of the shells has been reported previously,¹⁸ we present only the essential details here.

(26) Perez-Ruvalcaba, N. P.; Morales-Reyes, J. J.; Huitrn-Ramirez, J. A.; Rodriguez-Chagollin, J. J.; Rodriguez-Noriega, E. *Am. J. Med.* **1987**, *82*, 242–246.

(27) Davies, B. I.; Maesen, F. P. V.; Baur, C. *Eur. J. Clin. Microbiol.* **1986**, *5*, 226–231.

(28) Mortimer, P. G. S.; Piddock, L. J. V. *J. Antimicrob. Chemother.* **1991**, *28*, 639–653.

(29) Boas, F. E.; Forman, L.; Beutler, E. *Proc. Natl. Acad. Sci. U.S.A.* **1998**, *95*, 3077–3081.

(30) Pearce, B. E.; Wright, E. M. *Proc. Natl. Acad. Sci. U.S.A.* **1984**, *81*, 2223–2226.

(31) Postgate, J. R. In *Methods in Microbiology*; Norris, J. R., Ribbons, D. W., Eds.; Academic Press: London, 1969; Vol. 1.

(32) Glauret, A. M. *Practical methods in electron microscopy*; North-Holland Publishing Co.: Amsterdam, 1974.

(33) Hayat, M. A. *Principles and techniques of electron microscopy*; Van Nostrand Reinhold: New York, 1970.

(34) Sabatini, D. D.; Miller, F.; Bensch, K.; Barnett, R. J. *J. Histochem. Cytochem.* **1963**, *12*, 57–71.

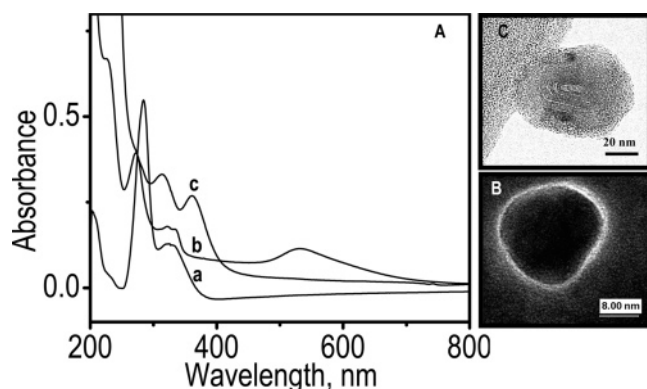


Figure 1. (A) UV-vis spectrum of (a) free ciprofloxacin, (b) Au@ciprofloxacin@SiO₂, and (c) cip@SiO₂. (B) shows an image of a Au@SiO₂ core-shell nanoparticle taken with an energy loss of 15 eV, and (C) shows the TEM image of the carbon onion structure formed inside the silica shell.

Free ciprofloxacin shows three characteristic absorption peaks in propanol as shown in Figure 1A (trace a), which match the features at 225, 283, and 326 nm reported in alkaline media.^{18,36} The absorption spectrum of Au@ciprofloxacin@SiO₂ shows the characteristic plasmon absorption band of gold nanoparticles apart from the three ciprofloxacin peaks (trace b). Cip@SiO₂ shows only the peaks due to ciprofloxacin (trace c). A red shift seen in the case of cip@SiO₂ is expected since many ciprofloxacin molecules are present inside the confined volume of the nanoshell. The surface of the gold nanoparticle used for the synthesis is covered with typically 585 molecules.¹⁹ A similar kind of red shift in the absorption spectrum is reported in the case of fluorescein isothiocyanate incorporated inside the nanoshell.³⁷

TEM images of the cip@SiO₂ nanoshells formed by the CN⁻ leaching method showed particles of average diameter ~15 nm, in agreement with the gold nanoparticles used in the synthesis (Supporting Information, p 2). The shell morphology is largely spherical as expected. The particles are extremely beam-sensitive, and they collapse upon prolonged exposure, which prevented detailed TEM examinations. Studies of dye incorporation inside the silica shell formed by the same method have also indicated nanoshells of similar dimensions.³⁷ Figure 1B shows Au@cip@SiO₂ core-shell particle imaged with an energy loss of 15 eV. The contrast is better here, and the shell completely surrounds the nanoparticles as shown. As these are the precursor species, it is reasonable to conclude that the shells are spherical. Nanoshells can also be obtained by the halocarbon mineralization³⁵ of the core by CCl₄. The shells obtained by this method³⁸ show carbon onion-like structures inside the silica shell as shown in Figure 1C. The presence of carbon has been confirmed by energy loss imaging as well.³⁸ The images show concentric structures of carbon with graphitic separation. Carbon is deposited as a result of the mineralization process.³⁸

The material has been characterized using fluorescence spectroscopy as well, and it showed a red-shifted peak at 458 nm as compared to 448 nm of free ciprofloxacin (Supporting Information, p 3). There was no fluorescence intensity for the supernatant when cip@SiO₂ was completely removed from the dispersion by centrifugation, showing that all the molecules are

Table 1. Minimum Inhibition Concentration of *E. coli* DH5 α and *L. Lactis* MG 1363 As Found by the Agar Dilution Method^a

strain used	MIC (μ g/mL)		
	ciprofloxacin	ciprofloxacin@SiO ₂	SiO ₂ nanoshells
<i>E. coli</i> DH5 α	1	0.75	no activity
<i>L. lactis</i> MG 1363	4	4	no activity

^a The uncertainty estimated in this study is less than 0.1 μ g/mL.

inside the shell. Further studies showed that the fluorescence anisotropy of cip@SiO₂ is around 0.1172 whereas for free ciprofloxacin it is 0.0560 in aqueous solution at room temperature. This indicates that cip@SiO₂ has less rotational freedom as compared to free ciprofloxacin, indicating that it is indeed inside the shell. In comparison, we note that 3-hydroxyflavone (3HF) in water at 35 °C shows anisotropy of 0.11 inside liposomes compared to 0.06 in the aqueous solution.³⁹

After characterization of the material using microscopy and different spectroscopic techniques, its antibacterial activity was looked at and was compared with that of free ciprofloxacin. The MIC is a measure to define the antibacterial activity of an organism and is defined as the lowest concentration of drug that inhibits visible growth.⁴⁰ The MICs obtained for *E. coli* DH5 α and *L. lactis* MG 1363 were found by the agar dilution method,³¹ and the data are presented in Table 1. They show the same value for the free drug and that incorporated within the nanoshell for *L. lactis*, while for *E. coli* there is a slight decrease in the latter, showing that ciprofloxacin@SiO₂ is a better antibacterial agent in the case of Gram-negative bacteria. In the control experiment using silica nanoshells without ciprofloxacin, no activity against both the organisms was seen (Table 1).

The antibacterial activity of an antibiotic depends both on its ability to pass through the cell envelope and also on its effective binding at the target site, in this case DNA gyrase.⁴¹ Since in this case the drug has been encapsulated, its ability to pass through the cell envelope has been modified. As the modified drug shows a better activity only in the case of Gram-negative bacteria, we suggest that the uptake mechanism may be modified (in comparison to that of the free drug). In the case of the Gram-negative organism, three different routes have been proposed for the penetration of fluoroquinolones through the cell envelope: (i) the hydrophilic pathway through the porin channels,⁴² (ii) the hydrophobic pathway through the membrane bilayer matrix,⁴³ and (iii) the self-promoted uptake pathway.⁴⁴ The first two entrance pathways would be influenced by the drug properties, such as hydrophobicity, size, and structure. The self-promoted uptake route is based on the displacement of divalent cations from the outer membrane lipopolysaccharides. Since the drug is incorporated inside a silica shell, it is likely that the drug may take a different pathway for penetration compared to the free fluoroquinolone.

To understand the uptake of cip@SiO₂ by the cell, accumulation as well as hydrophobicity studies of the material were carried out and compared with those of free ciprofloxacin.⁴⁵ To find the hydrophobicity of the material, its partition coefficient was determined in an octanol-water mixture.⁴⁶ A 0.1 M phosphate

(35) Nair, A. S.; Tom, R. T.; Suryanarayanan, V.; Pradeep, T. *J. Mater. Chem.* **2003**, *13*, 297–300.

(36) Wu, S.; Zhang, W.; Chen, X.; Hu, Z.; Hooper, M.; Hooper, B.; Zhao, Z. *Spectrochim. Acta* **2001**, *57*, 1317–1323.

(37) Imhof, J.; Megens, M.; Engelberts, J. J.; de Lang, D. T. N.; Sprink, R.; Vos, W. L. *J. Phys. Chem. B* **1999**, *103*, 1408–1415.

(38) Rosemary, M. J.; MacLaren, I.; Pradeep, T. *Carbon* **2004**, *42*, 2352–2356.

(39) Roy, O. S.; Mohanty, A.; Dey, J. *Chem. Phys. Lett.* **2005**, *414*, 23–27.

(40) Andrews, J. M. *J. Antimicrob. Chemother.* **2001**, *48*, 5–16.

(41) Lambert, P. A. *Adv. Drug Delivery Rev.* **2005**, *57*, 1471–1485.

(42) Nikaïdo, H.; Vaara, M. *Microbiol. Rev.* **1985**, *49*, 1–32.

(43) Kotera, Y.; Watanabe, M.; Yoshida, S.; Inoue, M.; Mitsuhashi, S. *J. Antimicrob. Chemother.* **1991**, *27*, 733–739.

(44) Chapman, J. S.; Georgopadakou, N. H. *Antimicrob. Agents Chemother.* **1988**, *32*, 438–442.

(45) Berlanga, M.; Montero, M. T.; Hernández-Borrell, J.; Viñas, M. *Int. J. Antimicrob. Agents* **2004**, *23*, 627–630.

(46) Fresta, M.; Wehrli, E.; Puglisi, G. *Pharm Res.* **1995**, *12*, 1769–1774.

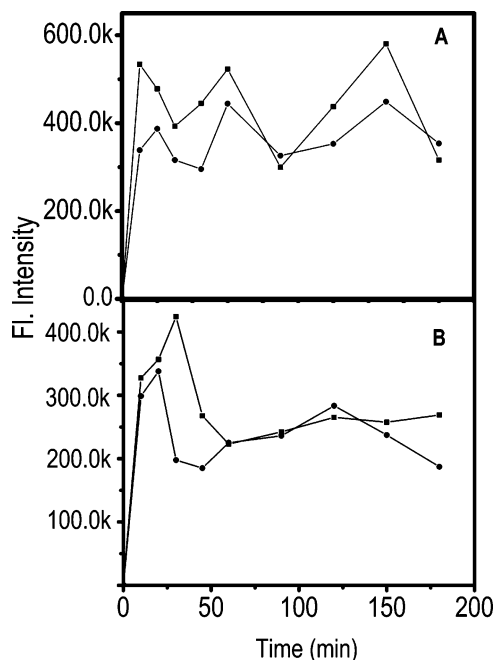


Figure 2. Fluorescent intensity profiles at 458 nm for ciprofloxacin (■) and cip@SiO₂ (●) for (A) *E. coli* DH5α grown in LB medium and for (B) *L. lactis* MG 1363 grown in M17 medium. The intensity fluctuation observed was under 10% in repeated measurements.

buffer (pH 7.2) saturated with 1-octanol was mixed with 1-octanol saturated with 0.1 M phosphate buffer (pH 7.2), 5 μg/mL of ciprofloxacin/ciprofloxacin@SiO₂ was added, and the resulting mixture was stirred for 12 h at room temperature. The partition coefficient is the ratio of the concentration of the compound present in the organic and aqueous phases. In the case of cip@SiO₂, it was found to be 0.913, whereas for free ciprofloxacin it was 0.505, indicating that cip@SiO₂ is distributed almost equally in the hydrophobic and hydrophilic phases. Thus, the difference between a free drug and cip@SiO₂ is that, after encapsulation, the hydrophobicity of the material changes, which affects the penetration and results in a decrease of the MIC for *E. coli*. In the case of Gram-positive bacteria, where there is no dependency on the penetration pathway, the encapsulation does not have much effect.

Accumulation studies were done on *E. coli* and *L. lactis* using ciprofloxacin and cip@SiO₂. It was found that the uptake of both the materials starts in the first 5 min of incubation and is greater for the free drug in comparison to cip@SiO₂ for a given interval of time (Figure 2). Uptake by *E. coli* is greater, considering the absolute intensities. The accumulation of drugs by an organism depends on the pH of the outer medium and also on the surface charge present on the cell membrane. It is found that⁴⁷ fluoroquinolones having a net charge are not passed through the cell membrane. The uncharged species is more likely to mediate passive diffusion. As the silica surface is hydrated with no net charge, the silica encapsulation can have the advantage of ensuring higher rates of drug entrance into the periplasmic space. Combined with the fact that cip@SiO₂ can pass through both hydrophilic and hydrophobic channels, as revealed by the partition studies, we conclude that better accumulation is possible in *E. coli*.

As we have seen from the above studies, ciprofloxacin incorporated inside a silica shell is released into the bacterial cell in both the cases of Gram-negative and Gram-positive organisms. Studies were conducted to image the distribution of the drug

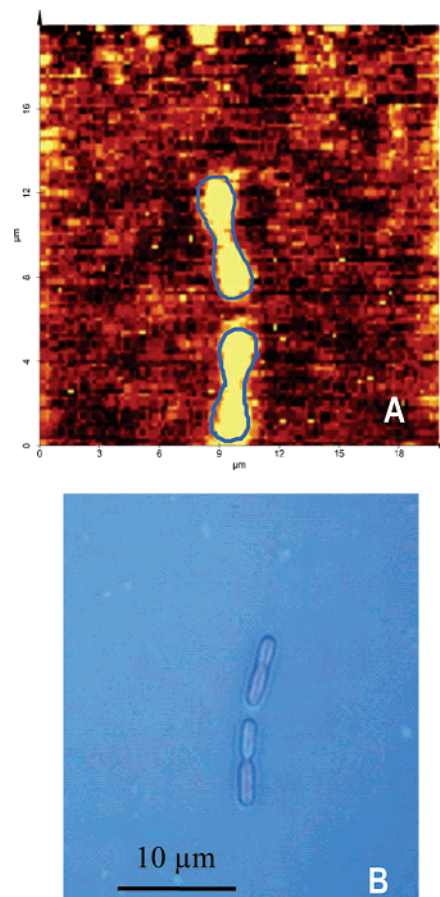


Figure 3. Fluorescence image of *E. coli* DH5α treated with FITC@SiO₂ (A) and the corresponding optical image (B). The bacterial contour is marked. The image corresponds to an area of 20 × 20 μm and was acquired in the spectrum imaging mode. Image A is slightly shifted vertically in comparison to the optical image. The two images appear different in orientation due to a change in the scan geometry.

inside the cell using the fluorescence imaging technique. We have done this study on *E. coli*. For the experiment, ciprofloxacin was replaced with FITC since it has been widely used for cell labeling and imaging. Cell imaging is usually used to find where molecules such as proteins, antibodies, and antibiotics go after entering the cell and how they are distributed inside.^{48,49} This can be done using many techniques, but fluorescence imaging is found to be very useful since it is simple and most of the dye molecules can be made to attach to proteins or antibodies using simple chemistry. Dyes which are used for this purpose are FITC, green fluorescent protein (GFP), and rhodamine isothiocyanate. In this particular study, FITC has been used, which has an excitation maximum around 495 nm (and can be excited by a 514.5 nm source) and an emission around 520 nm (and can be captured by the Raman microscope). Since it has an isothiocyanato group, it can be easily used for binding to the gold nanoparticle surface.⁵

We have synthesized FITC@SiO₂ as described in the case of cip@SiO₂ and incubated it with *E. coli* DH5α for 3 h. The pellet was washed to remove any surface-bound species, drop-cast on a glass slide, and analyzed as described above. The fluorescence image obtained is shown in Figure 3. As can be seen from the optical image (Figure 3B), most of the bacteria are ~2 μm in

(47) Furet, Y. X.; Deshusses, J.; Pechere, J. C. *Antimicrob. Agents Chemother.* **1992**, *36*, 2506–2511.

(48) Goldman, R. D.; Spector, D. *Live cell imaging: A laboratory manual*; CSHL Press: Cold Spring Harbor, NY, 2005.

(49) Geddes, C.; Lakowicz, J. R. *Who's who in fluorescence*; Springer: New York, 2003.

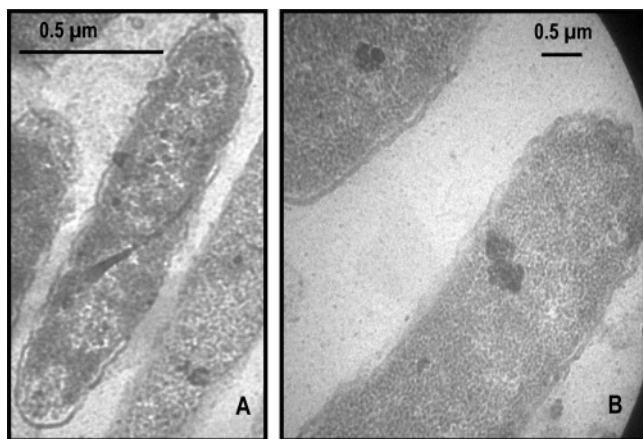


Figure 4. (A) TEM image of *E. coli* DH5α treated with cip@SiO₂. (B) Portion of a large bacterium.

length, but longer ones were also seen. The fluorescence image shows the contour of four organisms. As can be inferred from the image, FITC@SiO₂ enters the bacterial cell and is distributed uniformly. Note that the image was collected in the spectrum imaging mode with 10000 spectra in the 20 × 20 μm area. FITC@SiO₂ incubated with bacteria showed its characteristic emission feature when excited at 514.5 nm excitation (Supporting Information, p 4).

Transmission electron microscopy studies were also carried out on the bacteria incubated with cip@SiO₂ to probe the interaction of the bacterial cell after treatment with the SiO₂ nanoshell. Bacterial samples were washed and processed to get a resin block as explained in the Experimental Section. The 80 nm thick sections obtained were stained and imaged to find the difference in the bacterial structure after incubation with cip@SiO₂. Figure 4 shows the TEM images of *E. coli* treated with cip@SiO₂. The bacterial contour does not show any difference as a result of the nanoshell treatment. Nanoshells themselves were not detectable in the bacterial contour despite

repeated efforts (even at higher magnifications). It is likely that they collapsed within the organism or the electron beam destroyed them, considering their fragile nature. There is also a possibility of the shells being affected by the different chemical treatments that were carried out during the processing of the bacterial mass. Images of the parent *E. coli* are presented in the Supporting Information, p 4.

Conclusions

In conclusion, a silica-shell-based drug delivery system can improve the antibacterial property of loaded fluoroquinolone drugs, mainly due to the greater drug penetration within the bacterial cells. Drug delivery studies on cip@SiO₂ were carried out using *E. coli* DH5α and *L. lactis* MG 1363 by the agar dilution method, and the data were compared with those of free ciprofloxacin. Hydrophobicity studies on cip@SiO₂ suggest a different route of penetration for the material compared to the free drug. Interaction studies of the nanoshell with the bacteria were carried out using FITC@SiO₂, and the fluorescence image suggests that the shells go inside the organism. Transmission electron microscopy studies conducted on cip@SiO₂-treated *E. coli* suggest that the bacterial morphology is unaffected by the treatment with nanoshells, although the shells themselves were not detected.

Acknowledgment. T.P. thanks the Department of Science and Technology for financial support. Dr. Guhan Jayaraman and Mrs. Kalpana, Department of Biotechnology, IIT Madras, are thanked for allowing to use the laboratory facilities and also for their valuable suggestions. T. S. Sreepasad is thanked for help in the TEM measurements.

Supporting Information Available: Method of synthesis of silica nanoshells, TEM image of silica nanoshells, fluorescence excitation and emission spectra of cip@SiO₂, fluorescence spectrum of FITC@SiO₂-treated *E. coli* DH5α, and TEM images of free *E. coli* DH5α. This material is available free of charge via the Internet at <http://pubs.acs.org>.

LA061411H